Available online at www.sciencedirect.com
ScienceDirect
C. R. Chimie 10 (2007) 604–612
COMPTES RENDUS CHIMIE
http://france.elsevier.com/direct/CRAS2C/

Account / Revue

First critical steps for understanding complex advanced materials: Synergy between X-ray diffraction and electron microscopy

Maryvonne Hervieu*, Claude Michel

Laboratoire CRISMAT, UMR6508 CNRS/ENSICAEN, 6, bd du Maréchal-Juin, 14050 Caen cedex 4, France

Received 5 September 2006; accepted after revision 23 January 2007
Available online 8 March 2007

Abstract

Attaining novel structures in compounds displaying remarkable properties is the goal of numerous solid-state chemists and physicists. Several approaches for predicting new structures exist but, whatever they are, one of the essential steps is to understand their architecture. It needs to collect the maximum information for deciphering the building code. In this paper, we give a personal account and focus on the powerful synergy of transmission electron microscopy and X-ray diffraction techniques for achieving it. We have chosen the example of the misfit-layered cobaltites, which appear more and more complex as we attain each new level in the hierarchy of their structures. We have limited our illustration to the first period of the misfit cobaltites ''research story'', from the discovery of highly complex oxides to the understanding of the architecture building, without reporting on the numerous further papers devoted to iso-structural compounds and to their remarkable properties of thermoelectric power. ***To cite this article: M. Hervieu, C. Michel, C. R. Chimie 10 (2007).***

Résumé

La découverte de structures originales et de nouveaux matériaux à propriétés remarquables est le but de nombreux chimistes et physiciens du solide. Plusieurs approches permettent de tenter de prédire l'existence de telles structures, mais, quelle que soit la méthode utilisée, une des étapes essentielles est toujours de bien comprendre leur architecture. Dans cet article, nous présentons notre propre démarche en nous focalisant sur la puissance de la synergie entre la microscopie électronique en transmission et les techniques de diffraction des rayons X. Nous avons choisi l'exemple des cobaltites à structures lamellaires désaccordées, dans lesquelles chaque nouveau niveau de leur hiérarchie structurale dévoile une complexité croissante. Pour ce faire, nous avons limité notre illustration aux seuls débuts de l'histoire de ces matériaux complexes, de leur découverte à la compréhension de leur architecture, sans mentionner les nombreux articles, traitant de composés iso-structuraux, de leurs propriétés remarquables et de thermoélectricité, qui ont découlé de cette recherche fondamentale. ***Pour citer cet article : M. Hervieu, C. Michel, C. R. Chimie 10 (2007).***

Keywords: Research of new materials; Transmission electron microscopy; X-ray diffraction techniques

Mots-cléfs : Recherche de nouveaux matériaux ; Microscopie électronique en transmission ; Techniques de diffraction des rayons X

* Corresponding author.
E-mail address: maryvonne.hervieu@ensicaen.fr (M. Hervieu).

1631-0748/$ - see front matter © 2007 Académie des sciences. Published by Elsevier Masson SAS. All rights reserved.
doi:10.1016/j.crci.2007.01.011

1. Introduction

Every solid-state chemist agrees with the fundamental principle that a rational design of new materials is based on a deep understanding of the correlation between basic crystal chemistry and structure–property relationships. The discovery of potentially remarkable properties, either novel or of several orders higher levels, is of paramount importance in the context of a strong international competition. The improvement of the materials' performances is therefore a strong stimulus for determining the coupling between the external and internal structures, needing to control the maximum of chemical and physical factors, the new materials gaining then the status of "today's advanced materials".

Before the step of the delineation of the potential properties, the discovery of novel materials is often fed by the scientist's curiosity and needs determining the greater number of pieces that would allow the further building set. The story of the cuprates, complex oxides relatively unknown but high Tc superconductors-to-be, is one of the examples of these twenty last years, which had an unprecedented media impact and has, moreover, considerably improved the interactions between solid-state physic and material chemistry. The misfit structure of cobalt oxides, discovered in 1996, is another example of fundamental research, which leads up to a large structural family with a complex architecture and exceptional thermoelectric and magneto-transport properties. Following their discovery, a huge amount of work has been devoted to these now "today's advanced materials"; the global warming we nowadays live makes more than ever important the research of materials that can be involved in energy conversion. At the present time, the thermoelectric power value they can exhibit attains values higher than $+200\ \mu V\ K^{-1}$.

The aim of this paper is not to make a complete and detailed review on the thermoelectric misfit cobaltites–several have been already published–, but we do focus on the scope of the synergy between transmission electron microscopy (TEM) and X-ray powder diffraction (XRPD) techniques for determining the architectural bases of a new family, which will become the starting point of a new challenge of the solid-state physic and material chemistry.

2. State-of-the-art on two complex layered structures in 1996: misfit chalcogenides and RP's derivatives

The materials known as misfit-layer compounds have been firstly described by Mackovicky and Hyde [1] and a new class of chalcogenides, $(MX)_jTX_2$, was reported to adopt this structural mechanism [2–4]. One of the building pieces, the TX_2 layer, exhibits the CdI_2-type, which can be described as (111) rock salt (RS)-type layer made of an hexagonal arrangement of edge-sharing TX_6 octahedra (Fig. 1). The second one, (MX), is also a related rock salt (RS)-type layer, but (001) oriented, i.e. built up from distorted square pyramids MX_5.

The two types of layers, MX (sub-lattice S_1) and TX_2 (sub-lattice S_2), have different symmetries and the period along one in-plane direction are in an irrational ratio, resulting in a layer misfit and a stoichiometry different from the 1:1 ratio expected for a model of one MX layer alternating with one TX_2 layer along the perpendicular direction. The *j*-index, varying between 1.08 and 1.28, was used to denote both the mismatch and the stoichiometry of the compound.

For T = Ti, Nb, Ta [5], the possibility to add one extra octahedral TX_2 layer has been evidenced, leading to the formation of $(MX)_j(TX_2)_2$ members, with $j \approx 1.12–1.18$. Two important characteristics of these chalcogenides deserve to be highlighted. First, they exhibit intercalation properties as the parent structures (TX_2) and second, the structural mechanism can be compared to that observed for the members $m = 1$ and $m = 2$ of the $(AO)(ABO_3)_m$ Ruddlesden–Popper phases (Fig. 2a,b).

The intense research devoted to the copper oxides after the discovery of high Tc superconductivity (see Ref. [6] for review) allows the discovery of several families of novel cuprates, which are derivatives of the

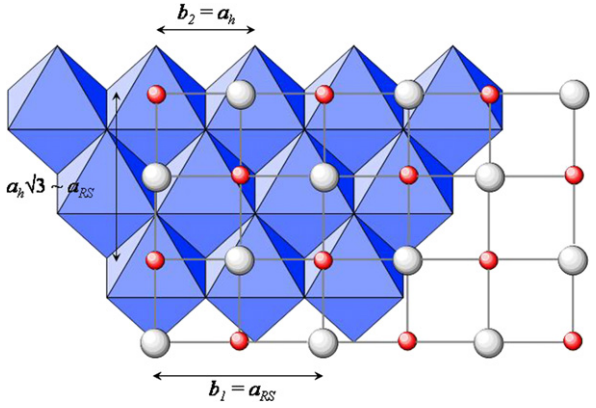

Fig. 1. In-plane view of the two superposed structures showing the lattice constant relationships. The blue octahedra adopt the pseudo hexagonal arrangement of the CdI_2-type layer and the red and white circles represent the cations and anions of one of the distorted RS layers. (For interpretation of the references to colour in this figure legend, the reader is referred to the web version of this article.)

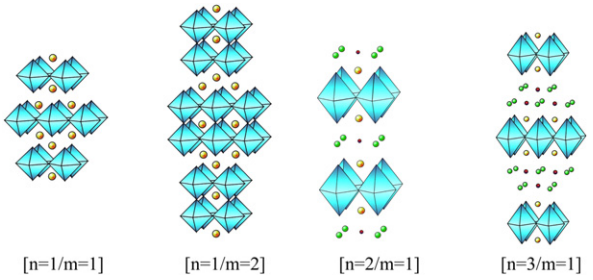

Fig. 2. Examples of different n and m members of the derivative Ruddlesden–Popper phases.

Ruddlesden–Popper (RP) phases. The intergrowth mechanisms of one RS layer with m perovskite-type layers have been extended and it was shown that the number of RS layers could also vary, following the general formulation $[AO]_n^{RS}[A'BO_3]_m^P$. The numbers $n = 1,2$ and 3 of RS layers with $m = 1,2,3,4$ of perovskite-type layers are observed in regular members exhibiting long-range intergrowth ordering along $\vec{c}$; note that non-integer n and m values are also observed in the form of more or less ordered polytypes. The structures of the members $[n = 1/m = 1]$, $[n = 1/m = 2]$, $[n = 2/m = 1]$ and $[n = 3/m = 1]$ are given in Fig. 2a,b,c and d, respectively.

The differences between the chalcogenides and the oxides have been previously described [7] in literature, including the two families of layered compounds, which are compared here. The high electronegativity and low polarizability of oxygen compared to the chalcogens imply more ionic metal–oxygen bonds, involving anionic repulsion between MO_2 layers, which hinder the stabilization of MO_2 layered oxides, contrary to the TX_2 layers. Accounting different parameters, the anticipations for the formation of similar misfit-layered oxides were not favourable.

3. The first layered misfit oxides

The first misfit-layered oxides were synthesized and studied in the laboratory by Boullay et al. in the system Tl–Ca–Sr–Co–O [8–11]. The starting idea [10] was the research of new layered oxides playing with three types of cations having different roles: the heavy d^{10} post-transition metals associated with alkaline earths (AE) could favour two-dimensional ordering, as observed in the $[AO]_n^{RS}[A'BO_3]_m^P$ phases, and transition metals could adopt mixed valences and different coordinations, mainly Co and Fe.

The powder X-ray diffraction patterns of the first syntheses clearly showed the formation of unknown phases, but the pattern matching attempts did not allow finding cell parameters. On the opposite, the electron diffraction (ED) techniques display patterns which can be directly interpreted as sections of the reciprocal space, so that we need only a small crystallite of the unknown structure for determining the cell parameters, without synthesizing a single-phased sample or growing a single crystal. The chemical analysis (cationic ratio) of the small crystallites is provided by energy dispersive spectroscopy (EDS).

These two important sets of data then allow looking for adequate synthesis process parameters and checking if the material is what one expects it is.

In the case of the cobaltites, the ED patterns clearly revealed the composite nature of the new phases (Fig. 3) since they are characterized by the superposition of two systems of reflections, as schematically represented in Fig. 3b. The orthorhombic rock salt-type layers is associated with the distorted sub-lattice S_1 (in blue) with $a_1 \approx 4.8$ Å and $b_1 \approx 4.5$ Å. (For interpretation of the references to colour, the reader is referred to the web version of this article.) It is superimposed to a second system exhibiting a pseudo-hexagonal symmetry ($a_h \approx 2.8$ Å, $\gamma \approx 120°$) and associated with the distorted sub-lattice S_2 (in red), corresponding to an orthorhombic double cell with $a_2 \approx 4.8$ Å and $b_2 \approx 2.8$ Å. The relationships between the parameters show that the two systems have a common a parameter but a different periodicity along $\vec{b}$, with $b_1 \approx 4.5$ Å and $b_2 \approx 2.8$ Å. These parameters suggested that one succeeded in the

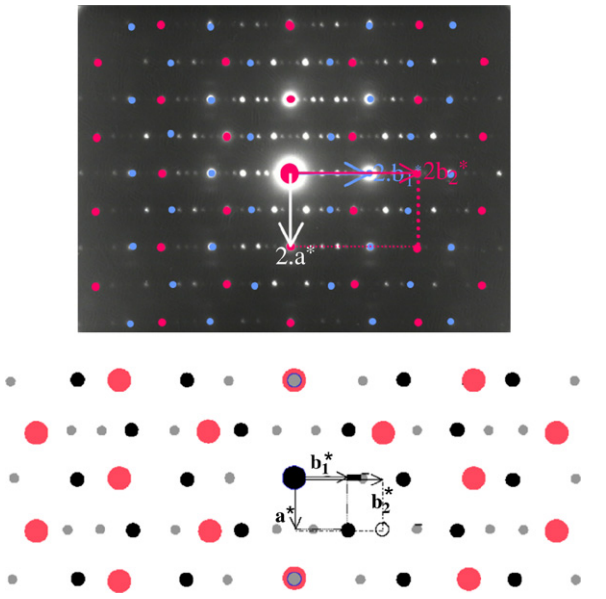

Fig. 3. Example of experimental and schematically drawn [001] ED pattern showing the two sub-lattices.

Table 1
Examples of cell parameters in the two classes of cobaltites with a "misfit" layered structure

System Bi–AE–Co oxides	System Tl–AE–Co oxides
Orthorhombic rock salt-type S_1: $a = 4.90$ Å, $b_1 = 5.11$ Å, $c = 29.86$ Å, $\beta = 93.4°$	Orthorhombic rock salt-type S_1: $a \approx 4.8$ Å, $b_1 \approx 4.5$ Å, $c \approx 10.8$ Å, $\beta \approx 98°$
Pseudo hexagonal double cell of S_2: $a = 4.90$ Å, $b_2 = 2.81$ Å, $c = 29.86$ Å, $\beta = 93.4°$	Pseudo hexagonal double cell of S_2: $a \approx 4.8$ Å, $b_2 \approx 2.8$ Å, $c \approx 10.8$ Å, $\beta \approx 98°$

synthesis of a misfit-type structure, with rock salt-type blocks associated with hexagonal (CoO_2) layers similar to those of $LiCoO_2$ and other $LiMO_2$ oxides (M = V, Cr, Ni [12]) crystallising in an $\alpha NaFeO_2$-type structure.

Due to their mica-like morphology, almost all of the crystallites are [001] oriented. The reciprocal space reconstructed by tilting around the crystallographic axes allows determining the symmetry and the periodicity of the stacking along the $\vec{c}$ direction. The cationic ratio of numerous crystallites, determined by EDS analyses, was systematically associated with the S_1 and S_2 parameters, determined by ED. Different systems have been investigated and a lot of compounds have been synthesized [10].

All are characterized by in-plane parameters of the same order (common a and different b_1 and b_2). The discordance between the two lattice parameters of the layer plane is, in both cases, clearly observed and easily calculated on ED patterns along the collinear $\vec{b}^*_1$ and $\vec{b}^*_2$ vectors. The b_1/b_2 ratio increases with the size of the alkaline earth and post-transition cations.

One of the key points deals with the periodicities along $\vec{c}$: first, the two different values of the c parameters showed that the oxides structures are different from those of the chalcogenides, implying a different stacking mode of the layers along $\vec{c}$ and, second, they allow characterizing two main groups of compounds, as exemplified in Table 1: the Bi-based ($c \approx 30$ Å) and the Tl-based cobaltites (c ≈ 11 Å).

However, besides these important results, the ED study revealed a high complexity of the structure.

3.1. The triple-rock salt-type blocks of the Bi-based cobaltites

The mismatch of the b_1 and b_2 parameters generates an incommensurate modulation, which is commonly called the "misfit modulation". However, in the case of the Bi-based cobaltites, it has been observed that a second incommensurate modulation characterized by a modulation vector $\vec{q} = 0.293\vec{a}^* + 0.915\vec{c}^*$ coexists with the "misfit modulation". It indeed considerably increases the difficulties for solving the structure. Understanding all the phenomena has needed synergy of two techniques: single-crystal X-ray diffraction and transmission electron microscopy. The refinement of the structure was carried out using the five-dimensional superspace-group formalism [13], in the superspace group $I2/a$ ($\alpha 0 \gamma$, $0 \mu 0$) pmm. This second modulation, called "intrinsic modulation", is associated with the Bi layers of the rock-salt block.

The structure of the Bi-based cobaltite is built up from the alternation of one distorted rock salt-type triple layers [$Bi_{1.74}Sr_2O_4$] (first sub-system) with a single [CoO_2] distorted CdI_2-type layer (second sub-system). The structure is drawn in Fig. 4, and the existence of four adjacent [AO] layers of the first sub-system is perfectly visible in high-resolution electron microscopy (Fig. 4b). In this image, the heavy electron density zones are highlighted so that four row of staggered

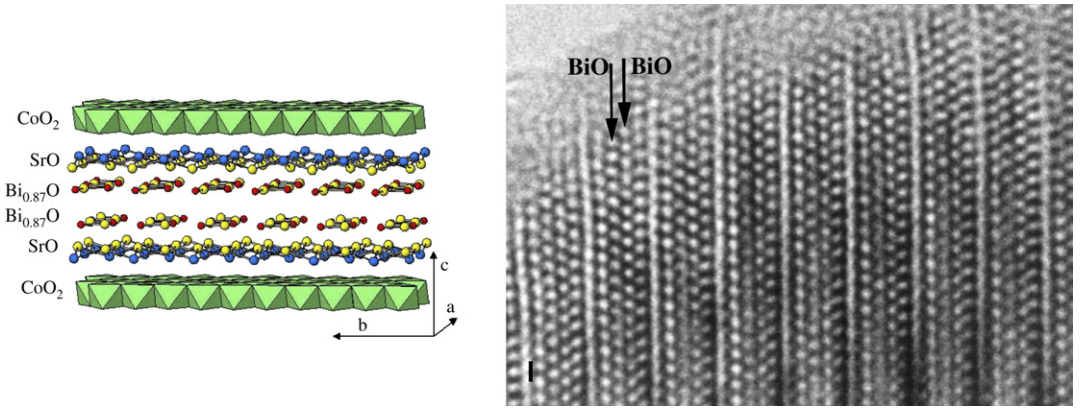

Fig. 4. Idealised drawing and HREM image of $[Bi_{1.74}Sr_2O_4][CoO_2]_{1.82}$.

bright dots are associated with four (AO) layers of a rock-salt structure. The $[CoO_2]$ layer appears as one row of narrow smaller bright dots.

The RS triple $[Bi_{1.74}Sr_2O_4]$ block results from the stacking of four layers according to the sequence $[(SrO)(Bi_{1-\delta}O)(Bi_{1-\delta}O)(SrO)]$. This RS block exhibits very close relationships with those observed in the Bi cuprates $Bi_{2-\delta}Sr_2CuO_6$ (Fig. 2d), by its ''intrinsic modulation'' (the second one) and the existence of disordered zones characterized by Bi vacancies regularly distributed in the $(Bi_{1-\delta}O)$ layers.

Note that, despite the ''mica-like'' character of the crystallite the chemical bonds between the Sr of the first sub-system and the O of the second sub-system are strong.

As a consequence of the differences between the chalcogenide $(MX)_j(TX_2)_n$ and cobaltite structures, a new denotation of the cobaltites was adopted for highlighting the two sub-systems. The misfit signature is outlined by the b_1/b_2 ratio, which is assigned to the single $[CoO_2]$ layer, whereas the number n of (AO) layers stacked to form the distorted rock salt-type block is denoted in more or less detailed ways.

So, the generic formulation adopted in the further studies is $[AO]_n[CoO_2]_{b_1/b_2}$, with a few variants as $[A_nO_n][CoO_2]_{b_1/b_2}$ and $[A_{n/2}O_{n/2}]_2[CoO_2]_{b_1/b_2}$, depending on the authors.

3.2. Double-rock salt-type blocks

The second series observed by Boullay [10] consists of numerous compounds with a cobaltite misfit-type structure exhibiting a periodicity along $\vec{c}$ close to 11 Å. As examples, this is the cases for the cation composition $Tl_\alpha(Sr_{1-y}Ca_y)_{1-\varepsilon}Co$ with $0 \le y \le 1$, $0.01 \le \alpha \le 0.35$, and the equivalent series with Pb and Hg and mixed $Pb_{0.6}Hg_{0.3}Sr_2Co_{1.77}$. The reconstruction of the reciprocal space allowed easily calculating the b_1/b_2 ratios and the periodicities along [001], the XRDP refining the parameters of the two sub-systems and EDS analyses determining the cationic ratio.

The absence of single crystals and the composite nature of the structure make difficult any structural determination, which needs in most cases the use of superspace groups. Even the calculation of the lattice constants of the two sub-lattices from the X-ray (or neutron) powder diffraction patterns is not trivial due to the superposition or the overlapping of a great number of diffraction lines of each sub-system and the presence, for $2\theta > 70°$, of a ''continuum'' of weak overlapped diffraction peaks, which makes virtually unusable this part of the pattern. Orientation phenomena highly possible due to the mica-like morphology of the crystallites and twinning phenomena evidenced by ED increase the difficulty to extract structural information.

One of the questions raised by these compounds was the appropriateness between the cationic ratio Tl + (Sr,Ca)/Co, the b_1/b_2 ratio, the c parameter and the formulation $[AO]_n[CoO_2]_{b_1/b_2}$. For solving the problem, we have selected a simplest formulation, i.e. α and $y = 1$, so that this cobaltite offered nice possibilities for studies combining electron microscopy and beam diffraction techniques, allowing to go ahead in the misfit-layered oxides.

3.2.1. $Ca_3Co_4O_9$ [14]

3.2.1.1. Electron diffraction and first images. Polycrystalline samples were obtained by heating in air at 900 °C for 24 h a mixture of CaO and Co_3O_4. The EDS analyses performed on numerous crystallites showed that the actual composition is close to the nominal one, Ca/Co ≈ 3/4. The oxygen analyses, using both thermal reduction and redox titration, converge to close results, i.e. ''$O_{9.07}$'' and ''$O_{9.02}$'', respectively, considering four cobalt atoms per formula unit. This oxygen content implies a composition close to $Ca_3Co_4O_9$ with a mean oxidation state close to +3 for cobalt.

The reconstruction of the reciprocal space from ED patterns (Fig. 5a and b) evidenced a composite structure characterized by the existence of two monoclinic subsystems having $\vec{a}^*$ as common axes and a misfit parameter along $\vec{b}^*$. The two sub-systems exhibit common a, c and β parameters and differ by the b axes (Table 1). Starting from these values, the lattice constant parameters were refined from the X-ray powder diffraction pattern: $a = 4.8376(7)$ Å, $b_1 = 4.5565(6)$ Å, $c = 10.833(1)$ Å, $\beta = 98.06(1)°$, $b_2 = 2.8189(4)$ Å, allowing the indexation of all diffraction peaks. The conditions limiting the intense reflections are $hk_20 (h + k_2 = 2n)$ and $hk_10 (h + k_1 = 2n)$.

Despite the a and b_1 parameters are directly correlated to the a_{RS} parameter of the rock salt (RS) structure, the a/b_1 ratio differs significantly from 1, implying a strong distortion of the RS sub-cell. Conversely the a/b_2 ratio, 1.716, remains close to $\sqrt{3}$, theoretical value for the hexagonal sub-system. The two sub-systems of reflections are clearly visible in the [001] ED patterns (Fig. 5a), whereas the hexagonal sub-system is also scarcely visible in the [010] patterns. Both exhibit great similarities with those of thallium and bismuth misfit oxides.

All these results were consistent with a structure closely related to that of Bi misfit-layered oxides, but the layer composition and stacking mode along the $\vec{c}$

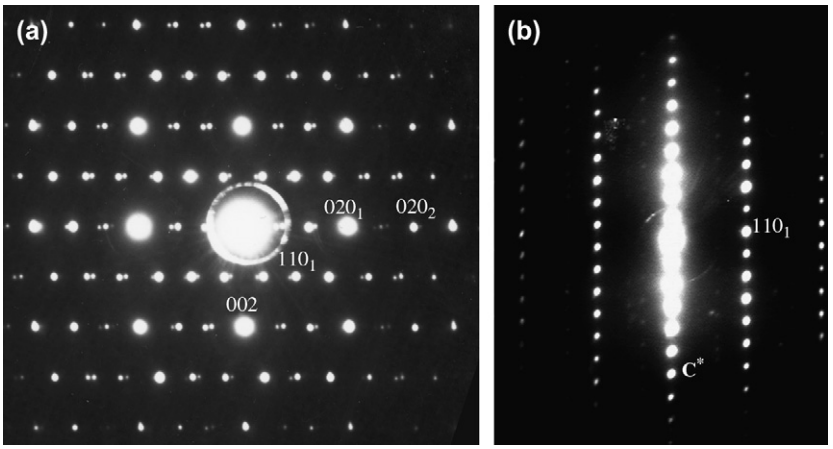

Fig. 5. (a) [001] and (b) [−110] ED patterns.

axis remained unknown. The nature of these layers strongly depends on the cationic composition, due to the possible mixed valence of the transition metal.

High-resolution electron microscopy (HREM) is a good tool for determining such stacking. The structure was explored viewing the crystals along [*hk*0] in order to identify the different layers. As shown in Fig. 6, a classical contrast was obtained along [100], for a focus value where the heavy electron density zones appear as bright dots (close to −55 nm). The contrast consists in three parallel rows of bright spots (indicated by three small black arrows), spaced by about 2.3 Å, instead of four in the Bi compounds (compare Fig. 4); they were then correlated to three (AO) layers. Between these groups, a row of weak and rather diffuse less bright dots is observed, which are correlated to the pseudo hexagonal (CoO_2) layer (white arrows).

The layer stacking mode consists of a triple $[AO]_\infty$ layer alternating with a single $[CoO_2]_\infty$ layer, with a high regularity as confirmed by all the [*hk*0] high-resolution images. The three $[AO]_\infty$ layers form a strongly distorted double RS-type slice associated with the first sub-system of reflections S_1. The single $[CoO_2]_\infty$ layer associated with the second sub-system is similar to that observed in A_xCoO_2 polytypes and in the Bi-based misfit cobaltites.

Considering the aforementioned formulation $[AO]_n[CoO_2]_{b_1/b_2}$, HREM showed that $n = 3$ and ED patterns that $b_1/b_2 = 4.557/2.819 \approx 1.613$ for the cationic Ca_3Co_4: one should admit that all the calcium and a part of cobalt are both present in this triple layer, involving a composition close to $[Ca_2CoO_3][CoO_2]_{1.61}$.

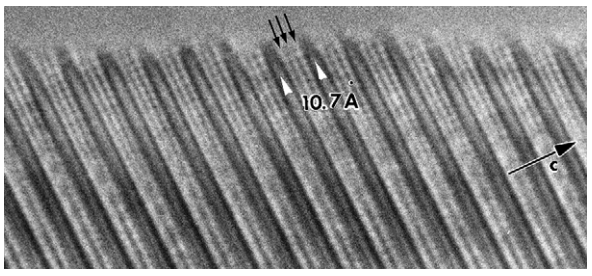

Fig. 6. [100] HREM images recorded for focus values close to −55 nm.

3.2.1.2. X-ray powder diffraction refinement. An accurate determination of such a complex structure was not realistic from powder diffraction data, but the structural information that could be extracted could be sufficient to give a good idea of the structure and, in particular, to confirm or invalidate the nature of the layers and their stacking mode. Accounting the ratio $b_1/b_2 = 1.613$, close to 13/8, a commensurate super-cell was considered in a first approximation with the lattice parameters: $a = 4.8376$ Å, $b = 36.479$ Å $\approx 8b_1 \approx 13b_2$, $c = 10.833$ Å, $\beta = 98.06°$. According to the supposed stacking sequence, this super-cell implies 26 CoO_2 units for the single $[CoO_2]_\infty$ layers and 16 Ca_2CoO_3 units for the triple $[AO]_\infty$ layers, i.e. the ideal composition $Ca_{32}Co_{42}O_{100}$. On the basis of steric considerations, one has assumed the layer succession "(CaO)−(CoO)−(CaO)" along $\vec{c}$ in the rock-salt block, as illustrated in Fig. 7. This ideal composition is close to the experimental one, in the limit of accuracy of the different techniques, and suggests a possible cation vacancy.

In order to move freely one sub-system with regard to the other, structural calculations were undertaken using *P*1 as tri-dimensional space group, which

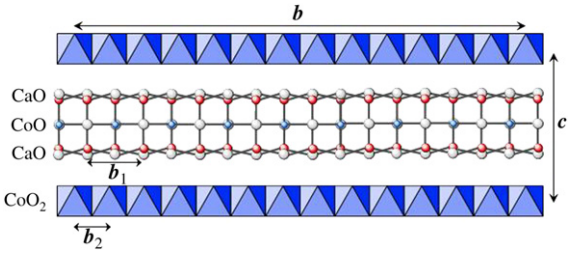

Fig. 7. Proposed structural model for "$Ca_3Co_4O_9$" involving a super-cell with $b \approx 8b_1 \approx 13b_2$.

involves 174 independent atoms in the super-cell. Starting from the above structural model and the ideal composition, constraints were applied to the coordinates of "equivalent" atoms in each sub-system, so that they vary with the same magnitude and allow reducing the number of variable parameters.

Under these conditions a R_{Bragg} factor of 20% was obtained. Despite high, such a value can be considered as a confirmation of the structural model if one accounts that the tri-dimensional approach, the ideal formula and the constraints to the atomic coordinates can only lead to an average solution.

Note that the presence of cobalt in the two types of layers implies two different sets of atomic bond distances, 1.8–1.9 Å in the $[CoO_2]_\infty$ layers, 2.2–2.4 Å in the $[AO]_\infty$ layers and can be related to different oxidation states, keeping in mind that the mean value is close to +3. By analogy with A_xCoO_2 polytypes, one can assume that the metallic conductivity measured for this oxide lies in the $[CoO_2]_\infty$ and is due to a mixed valence +3/+4 for cobalt. It would result in the presence of divalent cobalt in the intermediate $[CoO]_\infty$ layer sandwiched between the two (CaO) layers, in agreement with the longer interatomic Co–O distances.

3.2.1.3. Analysis of high-resolution images with the refined model. In high-resolution electron microscopy, the validation of one model can never be performed on the basis of a single image but needs the confrontation of experimental through focus series with calculated ones. One image of this series (Scherzer) can be directly interpreted in terms of projected potential, the heavy electron density zones appearing as dark dots. However, the other images are as important as the last-mentioned one, since provide essential information on different levels of the structure.

Thanks to the atomic positions obtained from the X-ray powder diffraction results the focus series was calculated, varying the focus values and crystal thickness. The [100] images calculated for a crystal thickness of 25 Å exhibit an average contrast in agreement with the experimental images. The good fit between calculations and experiment is an additional proof that this calcium cobaltite is a misfit-layered oxide which can be described by the formula which outlines the two sub-systems $[CoCa_2O_{3-x}][CoO_2]_{1.61}$.

However, a careful examination of the experimental images show, especially at the level of the intermediate layer of the rock-salt slice, contrast modulations, which cannot be simulated, whatever the focus and thickness values are in a general way, such contrast variation could be generated by non-stoichiometric phenomena and/or strong atomic displacements correlated to the presence of possible atom vacancies (both correspond to a decrease of the electron density in the theoretical atom positions) or to the mismatch between the two sub-systems. Due to the great number of variable parameters, it was impossible to account all the possible origins for image calculations, so one only considered the hypothesis of cobalt vacancies in the RS block, for testing the way they generate the perturbation of contrast.

The model used for image calculation is given in Fig. 8. A strong contrast modulation is observed along [001] in the experimental images (right part of Fig. 8) for focus values close to −550 Å. Along that direction, the contrast cannot be simply correlated to atomic rows, due to the complex superposition of the different layers along the viewing axis. The contrast variations calculated on the basis of the superstructure (left image of Fig. 8) are consistent with those observed in the experimental images.

4. The route was opened

The aim of this paper is to highlight the role of the synergy between transmission electron microscopy and X-ray powder diffraction techniques for determining the architectural bases of a new complex family, which could be the starting point of a new challenge of the solid-state physic and material chemistry. It is also to illustrate the results of a powerful daily synergy between synthesis, electron microscopy, powder and single-crystal X-ray diffraction techniques, each of them providing the accurate information for making step-by-step progress.

Within the context of research of layered cobaltites, these first studies, aiming at obtaining interesting properties on the bases of their bi-dimensional character and mixed valence of cobalt, were more fruitful than expected. From the fundamental point of view, they

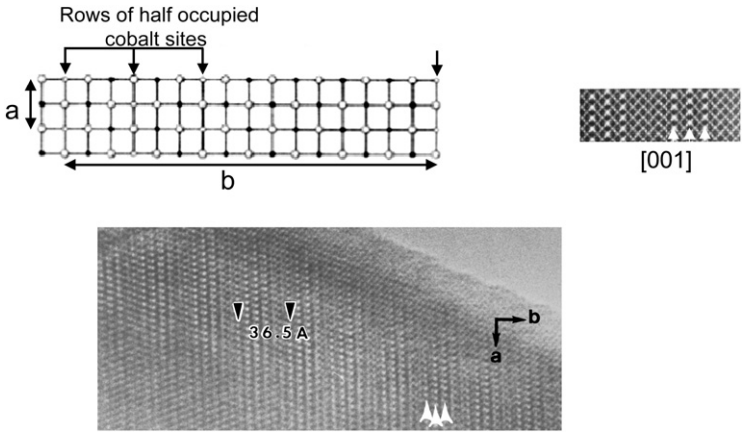

Fig. 8. Co deficient model: positions of the Co vacancies in the approximant, [001] calculated (left) and experimental [001] image recorded (right) for the corresponding focus value.

were the starting point of a large structural family with numerous members, as well as from the point of view of their properties, since they have already begun to be applied by different companies for their large thermopower values [15,16]. They have undoubtedly opened the route to a lot of new materials and to a wide field of chemical and physical researches. They also enlarge the number of parameters that one have to control for a rationally efficient improvement of the properties. Establishing the link between composition, structure and properties is not straightforward since parameters as ionic radius, charge and transition metal coordination interact concomitantly. The structural principle of the whole family is consistent with the aforementioned analysis on the higher electronegativity and low polarizability of oxygen with regard to chalcogenides. The more ionic metal–oxygen bonds, involving anionic repulsion between MO_2 layers, favour the stabilization of thicker RS blocks. The building mechanism of these structures presents interesting consequences. The first point deals with the formation of double (BiO) layers sandwiched between two (SrO) layers similar to those observed in the so-called 2201 and 2212 cuprates but this RS block appears in a layered arrangement different from that of the derivatives RP's phases. Another point is the existence of ''pure'' (CoO) layers sandwiched between two (SrO) or (CaO) layers in an RS-type block. Both effects allow enhancing knowledge of the blocks' inner architectures, which play a critical role in the properties of the bi-dimensional oxides, as cuprates and cobaltites.

The misfit cobaltites are now today's advanced materials and recent studies till provide a huge information on these materials, which will be certainly exploited to design new complex oxides ([17–21] only for examples, not an exhaustive bibliography). The route was not, by far, a dead end.

References

[1] E. Mackovicky, B.G. Hyde, Structure and Bonding, vol. 146, Springer-Verlag, Heidelberg, 1981, p. 101.
[2] G.A. Wiegers, A. Meetsma, S. van Smaalen, R.J. Haange, J. Wulff, T. Zeinstra, J.L. deBoer, S. Kuypers, G. Van Tendeloo, J. Van Landuyt, S. Amelinckx, A. Meerschaut, P. Rabu, J. Rouxel, Solid State Commun. 70 (1989) 409.
[3] G.A. Wiegers, A. Meerschaut, J. Alloys Compd. 178 (1992) 351.
[4] J. Rouxel, Y. Moëlo, A. Lafond, F.J. Disalvo, A. Meerschaut, R. Roesky, Inorg. Chem. 33 (1994) 3358.
[5] A. Meerschaut, L. Guemas, C. Auriel, J. Rouxel, Eur. J. Solid State Inorg. Chem. 27 (1990) 557.
[6] B. Raveau, C. Michel, M. Hervieu, D. Groult, Crystal Chemistry of High Tc Superconducting Copper Oxides, in: Springer Series in Materials Science 15, Springer-Verlag, 1991 (331 p.).
[7] J. Rouxel, Chem. Scr. 28 (1988) 33.
[8] P. Boullay, B. Domengès, M. Hervieu, D. Groult, B. Raveau, Chem. Mater. 8 (1996) 1482.
[9] P. Boullay, R. Seshadri, F. Studer, M. Hervieu, D. Groult, B. Raveau, Chem. Mater. 10 (1998) 92.
[10] P. Boullay, PhD Thesis, University of CAEN, 12/12/1997.
[11] M. Hervieu, P. Boullay, C. Michel, A. Maignan, B. Raveau, J. Solid State Chem. 142 (1999) 305.
[12] T.A. Hewston, B.L. Chamberland, J. Phys. Chem. Solids 48 (1987) 97.
[13] H. Leligny, D. Grebille, O. Perez, A.C. Masset, M. Hervieu, C. Michel, B. Raveau, C. R. Acad. Sci. Paris, Ser. IIc 2 (1999) 409.
[14] A.-C. Masset, C. Michel, A. Maignan, M. Hervieu, O. Toulemonde, F. Studer, B. Raveau, Phys. Rev. B62 (2000) 166.
[15] T. Itoh, T. Kawata, T. Kitajima, I. Terasaki, Int. Conf. Thermoelectr. Proc. 17 (1997) 595.

[16] A. Maignan, S. Hebert, L. Pi, D. Pelloquin, C. Martin, C. Michel, M. Hervieu, B. Raveau, Cryst. Eng. 5 (2002) 365.
[17] S. Li, R. Funahashi, I. Matsubara, K. Ueno, H. Yamada, J. Mater. Chem. 9 (1999) 1659.
[18] S. Li, R. Funahashi, I. Matsubara, K. Ueno, S. Soeeoka, H. Yamada, Chem. Mater. 12 (2000) 2424.
[19] M. Mikami, R. Funahashi, H. Yamada, Y. Mon, T. Sasaki, J. Appl. Phys. 94 (2003) 10.
[20] T. Yamamoto, K. Uchinokura, I. Tsukada, Phys. Rev. 65 (2002) 184434.
[21] H. Yamauchi, K. Sakai, T. Nagai, Y. Matsui, M. Karppinen, Chem. Mater. 18 (2006) 155.